

A compact system of small planets around a former red-giant star

S. Charpinet^{1,2}, G. Fontaine³, P. Brassard³, E. M. Green⁴, V. Van Grootel^{5,6}, S. K. Randall⁷, R. Silvotti⁸, A. S. Baran^{9,10}, R. H. Østensen¹¹, S. D. Kawaler¹⁰ & J. H. Telting¹²

Planets that orbit their parent star at less than about one astronomical unit (1 AU is the Earth–Sun distance) are expected to be engulfed when the star becomes a red giant¹. Previous observations have revealed the existence of post-red-giant host stars with giant planets^{2–4} orbiting as close as 0.116 AU or with brown dwarf companions^{5,6} in tight orbits, showing that these bodies can survive engulfment. What has remained unclear is whether planets can be dragged deeper into the red-giant envelope without being disrupted and whether the evolution of the parent star itself could be affected^{7–9}. Here we report the presence of two nearly Earth-sized bodies orbiting the post-red-giant, hot B subdwarf star KIC 05807616 at distances of 0.0060 and 0.0076 AU, with orbital periods of 5.7625 and 8.2293 hours, respectively. These bodies probably survived deep immersion in the former red-giant envelope. They may be the dense cores of evaporated giant planets that were transported closer to the star during the engulfment and triggered the mass loss necessary for the formation of the hot B subdwarf, which might also explain how some stars of this type did not form in binary systems.

KIC 05807616 (also known as KPD 1943+4058) is a seemingly isolated pulsating hot B subdwarf (sdB) star that has been monitored by the Kepler satellite primarily for the study of its oscillations^{10–12}. It is at an evolved stage of thermonuclear fusion of helium in its core, and belongs to the so-called extreme horizontal branch. This star shows a rich pulsation spectrum mostly composed of gravity (g-) modes^{13,14}. Its main structural parameters are well determined through asteroseismic means based on one month of Kepler exploratory data (Table 1)¹⁵. We focus here on additional Kepler time-series photometry obtained for this star after the exploratory phase.

The analysis of these data revealed many frequencies, most being associated with stellar oscillations (Fig. 1 and Supplementary Information section A1). However, we also found two very weak periodic modulations in the low-frequency range whose nature is most intriguing. The timescales involved for these variations are 5.7625 ± 0.0001 h (F_1 , with an amplitude of 52 ± 6 parts per million, p.p.m.) and 8.2293 ± 0.0003 h (F_2 , with an amplitude of ~ 47 p.p.m.; see Supplementary Information sections A2 and E). The phase folded curves show that these variations repeat at a coherent phase throughout the entire light curve (Fig. 1b and c). We determined that contamination from a nearby star, stellar pulsations, or rotational modulations (for example, through surface spots) cannot account for these variations, leaving orbital modulations as the most plausible interpretation (Fig. 1 and Supplementary Information sections B and C). Compact binary systems with an sdB star as the primary and having comparable orbital periods are indeed not atypical. However, in the present case, the very subtle modulations and the suggested presence of more than one companion raise the question of the

eventual substellar nature of these objects. In this context, the period ratio $F_2/F_1 \approx 1.43$, which is close to a 3:2 resonance, is also intriguing.

We explored this possibility by evaluating the properties (in particular the radius) that these objects would need to have in order to produce the observed variations in the light curve. There are two main sources of modulation involving small bodies. The first is reflection by

Table 1 | Derived parameters of KIC 05807616 and its two planet candidates

Stellar parameter ¹⁵	KIC 05807616	
Effective temperature, T_{eff} (K)	$27,730 \pm 270$	
Surface gravity, $\log[g]$ (c.g.s.)	5.52 ± 0.03	
Mass, M_* (M_{\odot})	0.496 ± 0.002	
Radius, R_* (R_{\odot})	0.203 ± 0.007	
Mean density, ρ_* (g cm^{-3})	84.1 ± 2.9	
Age after red-giant stage, A (Myr)	18.4 ± 1.0	
Bolometric luminosity, L (L_{\odot})	22.9 ± 3.1	
Apparent Johnson V-band magnitude, V	14.87 ± 0.02	
Distance from Earth, d (pc)	$1,180 \pm 95$	
Planetary parameter	Planet candidate 1 KOI 55.01	Planet candidate 2 KOI 55.02
Assumed Bond albedo [*] , α_j	0.10	0.10
Assumed temperature contrast [†] , β_j	0.2	0.2
Assumed inclination angle [‡] , i (degrees)	65	65
Assumed mean density [§] , ρ_j (g cm^{-3})	5.515	5.515
Orbital period, P_j (h)	5.7625 ± 0.0001	8.2293 ± 0.0003
Modulation amplitude, A_j (p.p.m.)	52 ± 6	~ 47
Orbit radius , a_j	8.9698×10^{10} cm	1.13749×10^{11} cm
	$1.290 R_{\odot}$	$1.636 R_{\odot}$
	0.0060 AU	0.0076 AU
Roche limit [¶] , d_R	0.0029 AU	
Mean temperature: day side [#] , T_j (K)	9,115	8,094
Mean temperature: night side [#] , T_j (dark) (K)	1,823	1,619
Planet radius [☆] , R_j (R_{\oplus})	0.759	0.867
Planet mass ^{**} , m_j (M_{\oplus})	0.440	0.655
Host star projected radial velocity ^{††} , v_j (m s^{-1})	0.65	0.86

Values shown assume the most probable configuration for this system. A third body (KOI 55.03) may be present between the two well secured detections (Fig. 1). If confirmed with more observations and using the same assumptions, its distance from the star would be 0.0065 AU, its radius 0.605 R_{\oplus} , its mass 0.222 M_{\oplus} , and its estimated temperature on the day (dark) side 8,735 K (1,747 K). Subscript @ indicates Earth value.

^{*} We use a low albedo value representative of hot Jupiters. This value is also close to Mercury's albedo. [†] $\beta = T_j(\text{dark})/T_j$ is a parametrization of the thermal imbalance on the planet surface. On Mercury, $\beta \approx 0.2$.

[‡] This inclination angle is suggested by the amplitude distribution of pulsation modes split by rotation. [§] Considering the derived radii, we assume rocky worlds with the Earth's density as a representative value.

^{||} Obtained from Kepler's third law (equation (D15), Supplementary information section D).

[¶] Distance from the star below which tidal disruption occurs (assuming a rigid body), $d_R \approx R_*(2\rho_*/\rho_j)^{1/3}$.

[#] Obtained assuming radiative equilibrium (equation (D5), Supplementary Information section D).

[☆] Derived from equation (D14) in Supplementary Information section D.

^{**} Derived from equation (D16) in Supplementary Information section D.

^{††} Derived from equation (D17) in Supplementary Information section D.

¹ Université de Toulouse, UPS-OMP, IRAP, F-31400 Toulouse, France. ² CNRS, IRAP, 14 avenue Edouard Belin, F-31400 Toulouse, France. ³ Département de Physique, Université de Montréal, CP 6128, Succursale Centre-Ville, Montréal QC H3C 3J7, Canada. ⁴ Steward Observatory, University of Arizona, 933 North Cherry Avenue, Tucson, Arizona 85721, USA. ⁵ Institut d'Astrophysique et de Géophysique, Université de Liège, 17 Allée du 6 Août, B-4000 Liège, Belgium. ⁶ FNRS, rue d'Egmont 5, B-1000 Bruxelles, Belgium. ⁷ ESO, Karl-Schwarzschild-Strasse 2, 85748 Garching bei München, Germany. ⁸ INAF-Osservatorio Astronomico di Torino, Strada dell'Osservatorio 20, 10025 Pino Torinese, Italy. ⁹ Mt Suhora Observatory, Cracow Pedagogical University, ulica Podchorzacych 2, 30-084 Krakow, Poland. ¹⁰ Iowa State University, Department of Physics and Astronomy, 12 Physics Hall, Ames, Iowa 50011, USA. ¹¹ Instituut voor Sterrenkunde, KU Leuven, Celestijnenlaan 200D, B-3001 Leuven, Belgium. ¹² Nordic Optical Telescope, Apartado 474, 38700 Santa Cruz de La Palma, Spain.

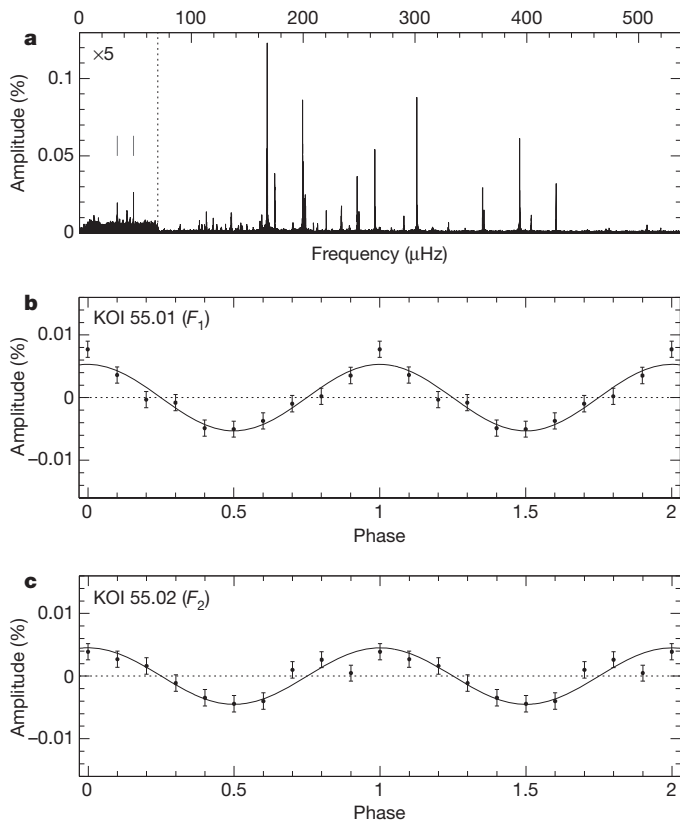


Figure 1 | Brightness variations detected in KIC 05807616. **a**, Amplitude spectrum of the light modulation; **b**, **c**, phase curves for the two planet candidates, KOI 55.01 (**b**) and KOI 55.02 (**c**). The combined Q2 + Q5–Q8 Kepler data (Qx refers to a 3-month observation quarter; see Supplementary Information section A1) have been used (that is, 14 months of monitoring spanning 21 months in total). In **a**, numerous peaks rising up to $\sim 0.15\%$ of the mean brightness of the star are due to g-mode pulsations (Supplementary Information section A1). Two weak variations indicated by vertical lines in the low frequency domain (shown with an amplitude expansion factor of 5) are also present, well disconnected from the g-modes. The frequency F_1 at $48.204 \pm 0.001 \mu\text{Hz}$ ($5.7625 \pm 0.0001 \text{ h}$) has a stable amplitude ($52 \pm 6 \text{ p.p.m.}$) and phase throughout the period of monitoring. F_2 at $33.755 \pm 0.001 \mu\text{Hz}$ ($8.2293 \pm 0.0003 \text{ h}$) is the dominant component of a more complex structure possibly caused by a frequency modulation (Supplementary Information sections A1 and E). After evaluating alternative interpretations (Supplementary Information sections B and C), we find that these structures are most likely to be the signatures of two bodies of substellar nature closely orbiting the star. We note that an even weaker signal between F_1 and F_2 (F_3 , $\sim 29 \text{ p.p.m.}$ at $42.4299 \mu\text{Hz}$ or 6.5467 h) could indicate the presence of a third body (KOI 55.03). In the following, we however concentrate on the two well secured detections. Panels **b** and **c** illustrate the light curve phase folded (in 10 phase bins) on the orbital period of KOI 55.01 (F_1) and KOI 55.02 (F_2), respectively (error bars, s.e.m.). These curves are obtained after ‘prewhitening’ the dominant g-mode pulsations. A small brightness excess occurring at phase zero in **b** is suggested. It may be typical of an opposition surge, but it is only a 1.9σ detection and more Kepler data will be needed to clearly establish its existence.

the surface of each planet of the light emitted by the star; such reflection would be modulated by the orbital motions, as we see the planets in different phases of illumination. The second source is a possible thermal imbalance between the heated day-side and cooler night-side hemisphere of each planet. Assuming the rotation of each planet is tidally synchronized to its orbital motion (a very likely situation for a compact system like KIC 05807616), we would see a thermal emission that was modulated along their orbits¹⁶. Both effects depend on unknown properties of the orbiting bodies. These are the amount of light reflected and absorbed at their surface (characterized by the Bond albedo, α) and how the absorbed heat is redistributed before being re-emitted. For this latter effect, we adopted a simple approach involving

average temperatures on the day and night sides, assuming radiative equilibrium and black-body re-emission. Heat redistribution is then characterized by a parameter, β , being the ratio of the mean temperature in the dark hemisphere to the mean temperature in the heated hemisphere. The magnitude of these variations also depends on the inclination angle of the system relative to the observer.

We calculated the planets’ properties as functions of the parameters mentioned above and explored all plausible situations (Supplementary Information section D). Our findings from this thorough analysis are as follows: (1) in all configurations except for very small inclination angles ($i < 20^\circ$), the derived radii for the orbiting objects are in the planetary range. (2) If efficient heat redistribution occurs ($\beta > 0.90$), the objects would be in the giant planet range of sizes, similar to Neptune or Jupiter in size. However, in most situations (when $\beta < 0.80$), the day/night temperature contrast effect dominates, and nearly Earth-sized planets are predicted. As this system is extremely compact and orbits a very hot star, the temperature contrast between the two hemispheres should be large, and therefore the value of β small, and the small-planet solution is preferred. (3) The assumed albedo has a limited influence on the above results and does not qualitatively change the conclusions. A low albedo, $\alpha \approx 0.10$, is generally observed for hot gaseous planets^{17–19} and Mercury, in our Solar System, has a comparable albedo (but, admittedly, it may not be representative of the hottest telluric worlds). The last unknown is the inclination angle of the system, and its effect is illustrated in Fig. 2. At very small inclinations ($i < 3^\circ$), the derived radius could still be in the giant-planet range. However, the pulsations detected in KIC 05807616 provide valuable indications that small angles ($i < 20^\circ$) are improbable, suggesting instead that $i \approx 65^\circ$. This additional constraint relies on the reasonable assumption that the orbits of the planets are most probably coplanar with the star’s equatorial plane (see Supplementary Information sections A3 and A4).

On the basis of these considerations, we have derived the parameters for the two planet candidates, named KOI 55.01 and KOI 55.02, from the most probable configuration for this system (Table 1). These parameters suggest that the two planets are smaller than Earth, which would make them the smallest planets so far found around a star still undergoing nuclear fusion. Considering their sizes and orbital parameters, their nature is most probably telluric. This conclusion may be further supported by a possible brightness excess (but only a 1.9σ detection at this stage) at phase zero in the phase curve of KOI-55.01 (Fig. 1). This excess, if real, could be associated with an opposition surge, a phenomenon observed with solid bodies having a tenuous (or no) atmosphere²⁰. The two planet candidates are also remarkable for the very high temperatures expected at their surfaces, indicating that they must be undergoing significant evaporation. However, these atypical properties, compared with those of known planets orbiting main-sequence stars, should not be surprising, considering the nature of the parent star. Planets in extreme environments have been reported previously²¹.

Our two planets were most probably swallowed by their parent star when it became a red giant, a stage that ended only ~ 18 million years ago¹⁵. They were probably orbiting further away and may have been dragged deep into the red-giant envelope to their current positions²². The fact that they are of equivalent size with orbits close to a 3:2 resonance may be an important factor explaining their survival. Indeed, preliminary *N*-body calculations (not shown) suggest that this system is dynamically stable, as long as the planet masses remain lower than several Earth masses; the system may also be stable when a third small planet is present between KOI 55.01 and KOI 55.02. This is consistent with our finding that small bodies should be involved.

This discovery suggests that planets may influence stellar evolution⁹. The increased envelope mass ejection required to form sdB stars from red giants is expected to occur in close interacting binaries, where the companion can transfer some of its orbital momentum to the expanded red-giant envelope, speeding up its rotation and thus triggering its enhanced dissipation²³. However, this does not explain how about half

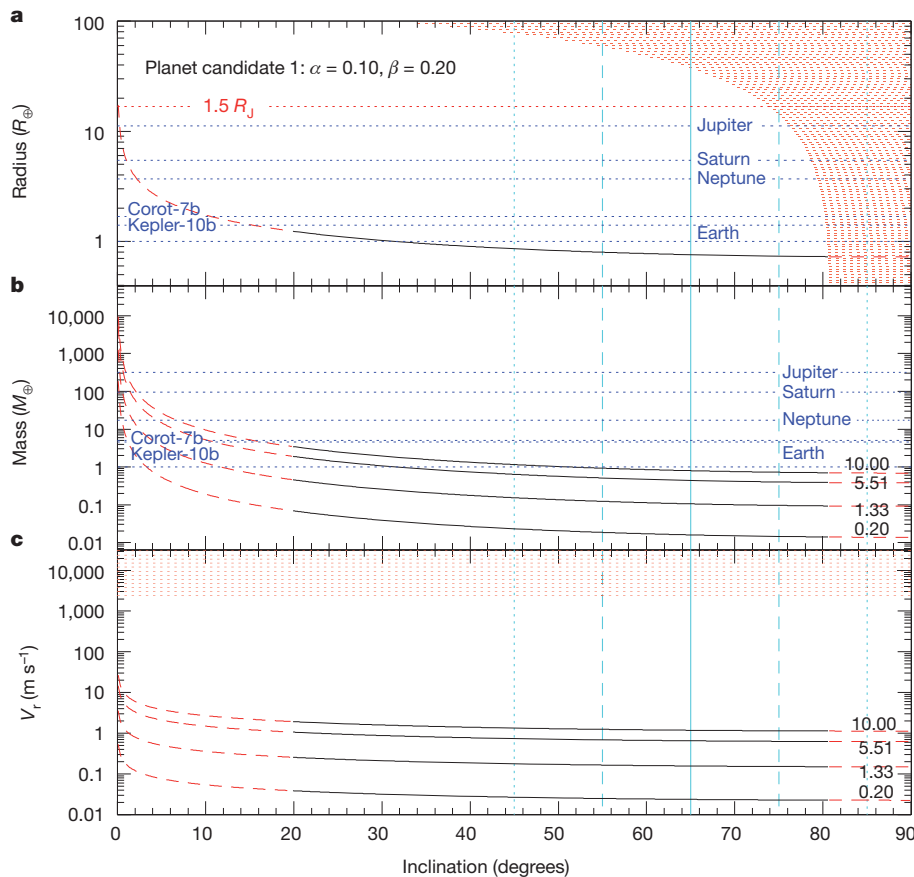


Figure 2 | The calculated properties of the first planet candidate (KOI 55.01) depend on the inclination of the system. Shown are the inclination dependence of the estimated radius (a; in Earth radii, R_{\oplus}), the estimated mass (b; in Earth masses, M_{\oplus}) and the host star projected radial velocity modulation (c; V_r , in m s^{-1}) as functions of the inclination. We assume representative values for the Bond albedo ($\alpha = 0.10$) and the average temperature contrast between the night and day sides ($\beta = 0.2$; that is, approximately the contrast observed on Mercury). The β -parameter strongly depends on the efficiency of heat redistribution on the planet's surface and, consequently, on the presence or absence of an atmosphere. A hot Jupiter with efficient heat redistribution has indeed been found: HD189333b, which, unlike Mercury, has a measured β of 0.8 (ref. 16). However, the precise value of β has a limited impact, as long as $\beta < 0.8$ (Supplementary Information section D). The red filled regions (and dashed portions of the curves) shows excluded domains due to the absence of eclipses (at large inclinations), due to our current upper limit on projected radial velocity modulations (2.4 km s^{-1} at 2σ ; Supplementary Information section C5), and due to asteroseismic indications rejecting an inclination angle

of the sdB stars that, like KIC 05807616, appear to be single or in well detached binaries²⁴, could be produced. In the present case, the planets may have contributed to the dissipation of the envelope to the point of making KIC 05807616 become an extreme horizontal branch star instead of a normal horizontal branch star with a thicker residual envelope²⁵. A plausible scenario would be that these bodies were originally giant planets immersed in the red-giant envelope and massive enough to survive engulfment and trigger the enhanced mass loss necessary for the formation of a hot B subdwarf star²⁶. During that episode, the planets may have been stripped down, losing their gaseous layers and being left only with their inner rocky/iron cores, which would be exposed. The small detected bodies would then be these cores, also named Chthonian planets²⁷, which are dense enough to lie beyond their Roche limit (see Table 1), thus avoiding disruption by the strong tides generated by the parent star.

Alternative scenarios may also be considered. Another way to form single sdB stars is through the merger of two helium white dwarfs²³, and planet formation following this event may be possible²⁸. We could

lower than $\sim 20^\circ$, instead suggesting that $i \approx 65^\circ \pm 10^\circ$. This last constraint is indicated by the light-blue vertical lines that show the expected angle (65° , solid line) with its approximate 1σ (dashed lines) and 2σ (dotted lines) ranges (Supplementary Information section A4). The radii and masses of Jupiter, Saturn, Neptune, Corot-7b²⁹ and Kepler-10b³⁰, are indicated for comparison purposes (dark-blue dotted horizontal lines). We also indicate the limit of $1.5R_J$ (R_J , Jupiter's radius; the red dotted horizontal line in a). Four different curves are shown for the mass and projected radial velocity estimations which sample the typical range of density, ρ_p , where extrasolar planets are usually found. The values $\rho_p = 5.51 \text{ g cm}^{-3}$ and $\rho_p = 1.33 \text{ g cm}^{-3}$ correspond to the mean density of Earth and Jupiter, respectively. With all these considerations, the most likely solution for the planetary parameters clearly points towards planets slightly smaller than our Earth, and therefore most probably of a solid nature (hence with a high mean density; see Table 1). A dynamical confirmation through a measurement of the projected radial velocity of the host star remains difficult at this stage for this relatively faint ($V = 14.87 \text{ mag}$) star, but may be possible with the next generation instrumentation.

speculate that the collapse of the extended envelope resulting from this merger could produce a circumstellar disk, where second generation planets may form. However, it seems unlikely that new, sufficiently dense, planets could have formed within a rather short period of time (less than $\sim 18 \text{ Myr}$) in an environment that close to this hot star.

Received 6 July; accepted 13 October 2011.

1. Udry, S. & Santos, N. C. Statistical properties of exoplanets. *Annu. Rev. Astron. Astrophys.* **45**, 397–439 (2007).
2. Setiawan, J. *et al.* A giant planet around a metal-poor star of extragalactic origin. *Science* **330**, 1642–1644 (2010).
3. Silvotti, R. *et al.* A giant planet orbiting the 'extreme horizontal branch' star V391 Pegasi. *Nature* **449**, 189–191 (2007).
4. Lee, J. W. *et al.* The sdB+M eclipsing system HW Virginis and its circumbinary planets. *Astron. J.* **137**, 3181–3190 (2009).
5. Maxted, P. F. L., Napiwotzki, R., Dobbie, P. D. & Burleigh, M. R. Survival of a brown dwarf after engulfment by a red giant star. *Nature* **442**, 543–545 (2006).
6. Geier, S. *et al.* Binaries discovered by the MUCHFUSS project: SDSS J08205+0008 — an eclipsing subdwarf B binary with a brown dwarf companion. *Astrophys. J.* **731**, L22–L26 (2011).

7. D'Cruz, N. L., Dorman, B., Rood, R. T. & O'Connell, R. W. The origin of extreme horizontal branch stars. *Astrophys. J.* **466**, 359–371 (1996).
8. Heber, U. Hot subdwarf stars. *Annu. Rev. Astron. Astrophys.* **47**, 211–251 (2009).
9. Soker, N. Can planets influence the horizontal branch morphology? *Astron. J.* **116**, 1308–1313 (1998).
10. Gilliland, R. L. *et al.* Kepler asteroseismology program: introduction and first results. *Publ. Astron. Soc. Pacif.* **122**, 131–143 (2010).
11. Østensen, R. H. *et al.* First Kepler results on compact pulsators – I. Survey target selection and the first pulsators. *Mon. Not. R. Astron. Soc.* **409**, 1470–1486 (2010).
12. Reed, M. D. *et al.* First Kepler results on compact pulsators - III. Subdwarf B stars with V1093 Her and hybrid (DW Lyn) type pulsations. *Mon. Not. R. Astron. Soc.* **409**, 1496–1508 (2010).
13. Green, E. M. *et al.* Discovery of a new class of pulsating stars: gravity-mode pulsators among subdwarf B stars. *Astrophys. J.* **583**, L31–L34 (2003).
14. Charpinet, S. *et al.* Progress in sounding the interior of pulsating hot subdwarf stars. *AIP Conf. Proc.* **1170**, 585–596 (2009).
15. Van Grootel, V. *et al.* Early asteroseismic results from Kepler: structural and core parameters of the hot B subdwarf KPD 1943+4058 as inferred from g-mode oscillations. *Astrophys. J.* **718**, L97–L101 (2010).
16. Knutson, H. A. *et al.* A map of the day-night contrast of the extrasolar planet HD 189733b. *Nature* **447**, 183–186 (2007).
17. Snellen, I. A. G., Mooij, E. J. W. & Albrecht, S. The changing phases of extrasolar planet CoRoT-1b. *Nature* **459**, 543–545 (2009).
18. Leigh, C. *et al.* A new upper limit on the reflected starlight from τ Bootis b. *Mon. Not. R. Astron. Soc.* **344**, 1271–1282 (2003).
19. Rowe, J. F. *et al.* The very low albedo of an extrasolar planet: MOST space-based photometry of HD209458. *Astrophys. J.* **689**, 1345–1353 (2008).
20. Mallama, A. Characterization of terrestrial exoplanets based on the phase curves and albedos of Mercury, Venus and Mars. *Icarus* **204**, 11–14 (2009).
21. Wolszczan, A. & Frail, D. A. A planetary system around the millisecond pulsar PSR1257 + 12. *Nature* **355**, 145–147 (1992).
22. Villaver, E. & Livio, M. The orbital evolution of gas giant planets around giant stars. *Astrophys. J.* **705**, L81–L85 (2009).
23. Han, Z. *et al.* The origin of subdwarf B stars – I. The formation channels. *Mon. Not. R. Astron. Soc.* **336**, 449–466 (2002).
24. Maxted, P. F. L. *et al.* The binary fraction of extreme horizontal branch stars. *Mon. Not. R. Astron. Soc.* **326**, 1391–1402 (2001).
25. Bear, E. & Soker, N. Connecting planets around horizontal branch stars with known exoplanets. *Mon. Not. R. Astron. Soc.* **411**, 1792–1802 (2011).
26. Nordhaus, J. *et al.* Tides and tidal engulfment in post-main-sequence binaries: period gaps for planets and brown dwarfs around white dwarfs. *Mon. Not. R. Astron. Soc.* **408**, 631–641 (2010).
27. Hébrard, G., Lecavelier Des Étangs, A., Vidal-Madjar, A., Désert, J.-M. & Ferlet, R. Evaporation rate of hot Jupiters and formation of chthonian planets. *ASP Conf. Proc.* **321**, 203–204 (2004).
28. Silvotti, R. The subdwarf B + giant planet system V391 Peg: Different scenarios for its previous evolution. *ASP Conf. Ser.* **392**, 215–219 (2008).
29. Léger, A. *et al.* Transiting exoplanets from the CoRoT space mission. VIII. CoRoT-7b: the first super-Earth with measured radius. *Astron. Astrophys.* **506**, 287–302 (2009).
30. Batalha, N. M. *et al.* Kepler's first rocky planet: Kepler-10b. *Astrophys. J.* **729**, 27–47 (2011).

Supplementary Information is linked to the online version of the paper at www.nature.com/nature.

Acknowledgements S.C. thanks the Programme National de Physique Stellaire (PNPS, CNRS/INSU, France) for support. G.F. acknowledges the support of the NSERC of Canada and the contribution of the Canada Research Chair Program. MMT spectra for KIC 05807616 were obtained at the MMT Observatory, a joint facility of the University of Arizona and the Smithsonian Institution. A.S.B. acknowledges funding from the Polish Ministry of Science and Higher Education. S.C. thanks R. Gilliland for help in managing Kepler's procedures. We acknowledge the Kepler team and all who have contributed to making this mission possible. Funding for the Kepler mission is provided by NASA's Science Mission Directorate.

Author Contributions S.C. wrote the manuscript, and analysed and interpreted the data from which the presence of planetary bodies was inferred. S.C., G.F., P.B. and V.V.G. derived and checked the calculations to estimate the planets' properties. G.F., P.B. and S.K.R. computed the cut-off frequencies and the theoretical mode visibilities based on a model of the star from V.V.G. E.M.G. obtained and analysed radial velocity measurements. S.D.K., A.S.B., R.H.Ø, R.S. and J.H.T. from the KASC WG11 group independently checked the detection of the orbital signals in the data. All authors discussed the results and contributed to their interpretation.

Author Information Reprints and permissions information is available at www.nature.com/reprints. The authors declare no competing financial interests. Readers are welcome to comment on the online version of this article at www.nature.com/nature. Correspondence and requests for materials should be addressed to S.C. (stephane.charpinet@ast.obs-mip.fr).